

The lattice constants used in this program are always transformed so as to name the actual rotation axis 'c'. All v and φ angles are given to the nearest 0.01° , then multiplied by 100 to convert the angle to integer form. The first section of PEXRAD INPUT systematically generates by l th layers all the combinations of $\pm h, \pm k, l$ which are permitted by the restrictions on μ and by the space group. The angle μ for a given crystal varies only with l , so that the value of l hence determines v_{\max} . The angles v_j for the allowed $(hkl)_j$ reflections in each l th layer, already computed in the test on v_{\max} , are stored and the corresponding φ_j angles are then computed. PEXRAD INPUT now orders the $(hkl)_j$ points (for each successive l th layer) to make $|v_{j+1} - v_j| + |\varphi_{j+1} - \varphi_j|$ a minimum. The reciprocal lattice point for which $v_j + \varphi_j$ is smallest is chosen as $(hkl)_1$, the starting point. This criterion applies to PEXRAD since the v and φ shafts rotate with equal angular velocity. At the same time the $(hkl)_j$ points are ordered, the corresponding rotation sense between the j th and $(j+1)$ th point is computed for v and φ . The output from this program is printed and put on punched cards. The punched cards are used to produce the paper tape input to PEXRAD. The output includes μ (for each l th layer) followed by $(hkl)_j, v_j + v_0$, rotation sense of v -shaft, $\varphi_j - \Delta\varphi + \varphi_0$, sense of φ -shaft, $\Delta'\varphi, \varphi_j + \Delta\varphi + \varphi_0$, and sense of φ -shaft.

Communication with PEXRAD is accomplished by means of perforated 5-channel paper tape. The format required by the records on these tapes imposes format restrictions on the punched cards from PEXRAD INPUT. Standard output formats are inadequate. A separate output program was written in FAP to provide the punched cards in the correct format.

Logic of PEXRAD OUTPUT program

PEXRAD OUTPUT is designed to check the performance of PEXRAD and then to compute the fully corrected structure factors from the integrated intensity of each measured reflection. The three angles $v + v_0, \varphi - \Delta\varphi + \varphi_0$ and $\varphi + \Delta\varphi + \varphi_0$ (Fig. 1) defining each reflection, actually reached and recorded by the diffractometer, are compared with the computed values. Differences of more than 0.02° are indicated as described in the following section. The succeeding $(2\Delta\varphi/\Delta'\varphi) + 1$ intensity values N_j , which comprise the profile through the reciprocal lattice point in a direction across the central lattice line, are scanned for statistical and other errors. Such errors are indicated in the printout.

The numerical value of each intensity in counts per second is then replaced by the corresponding value from a 'linearity' table. This is an experimentally determined table of true count rate *versus* recorded count rate. Differences are caused by 'dead-time' losses in the count system of about $1 \mu\text{sec}$

(Abrahams, 1962). The area under this corrected profile is calculated from the expression:

$$I(hkl) = \frac{\Delta'\varphi}{t} \left\{ \sum_1^K N_j - \frac{K}{20} \left[\sum_1^{10} N_j + \sum_{K-9}^K N_j \right] \right\},$$

where t is the present time in seconds for each intensity count, and the second and third summation terms sample the background, provided that neither term contains any trend that would vitiate their use for background measurement. The presence of such a trend is detected and a comment is printed. The variance in the resulting integrated intensity is taken to be:

$$\sigma^2(I(hkl)) = \left[\frac{\Delta'\varphi}{t} \right]^2 \left\{ \sum_{11}^{K-10} N_j + \left(\frac{K}{20} - 1 \right)^2 \left[\sum_1^{10} N_j + \sum_{K-9}^K N_j \right] \right\}.$$

In case $I(hkl) \leq 3\sigma(I(hkl))$, the value $3\sigma(I(hkl))$ is substituted for $I(hkl)$. This estimated intensity is preceded by a special symbol on the printout to show that this value is greater than or equal to the true but not measurable intensity.

The integrated intensity $I(hkl)$, and the standard deviation in this intensity (assuming the only source of error to be a Poisson distribution in each N_j) are corrected for absorption, A , extinction, E , and the Lorentz, L , and polarization, p , factors. The absorption correction is obtained by a machine integration of

$$A = \frac{1}{V} \iiint \exp[-\mu(p+q)] dx dy dz \quad (\text{Bond, 1959})$$

at 5° θ -intervals. In this integration, the μR of the actual crystal is used, and the value of A for a given θ is obtained by interpolation (Sautter, 1961). At present, the extinction correction is replaced by unity. The final structure factor is calculated as

$$F(hkl) = [I(hkl)/A.E.L.p]^{\frac{1}{2}}$$

and the standard deviations in $F^2(hkl)$ and $F(hkl)$ as

$$\sigma(F^2(hkl)) = \sigma I(hkl)/A.E.L.p$$

and

$$\sigma(F(hkl)) = \sigma(F^2(hkl))/2F(hkl).$$

Outline of PEXRAD OUTPUT program

The input data for this program include a table of absorption correction factors *versus* Bragg angle. A separate program† is used to produce this table (Sautter, 1961). This is followed by a character card containing the symbols used as error flags in the final printout. Next are tables of corrected and the corresponding uncorrected intensities, on a count per second basis, followed by a title card, a^*, b^*, c^* ,

† This table need be computed once only for a given crystal and then used repeatedly with successive sets of data from that crystal in PEXRAD OUTPUT.

$\cos \alpha^*$, $\cos \beta^*$, $\cos \gamma^*$, φ_0 , v_0 , $\Delta\varphi$, $\Delta'\varphi$ and t . Finally PEXRAD OUTPUT reads the data from PEXRAD. Each record of PEXRAD data contains $(hkl)_j$, $v_j + v_0$, $\varphi_j - \Delta\varphi + \varphi_0$, K values of N_j and $\varphi_j + \Delta\varphi + \varphi_0$. These data are converted from paper tape to punched cards for processing by PEXRAD OUTPUT.†

PEXRAD OUTPUT calculates $v_j + v_0$, $\varphi_j - \Delta\varphi + \varphi_0$, and $\varphi_j + \Delta\varphi + \varphi_0$ from the observed $(hkl)_j$ using the same formulae as in PEXRAD INPUT. Differences between observed and calculated angles of more than 0.02° are recorded on a separate magnetic tape. All such angle errors are collected and printed out at the conclusion of PEXRAD OUTPUT, and the hkl entry in the final printout is preceded by *. A final angular check is the determination of the position of the maximum N_j . The difference between the position of the maximum and the theoretical midpoint is given in the printout in units of $\Delta'\varphi$.

In the intensity error check, the N_j 's are scanned and all the remaining maxima and the minima are collected. Each such N_j is then compared with $(N_{j-1} + N_{j+1})/2$. If the resulting difference exceeds 6σ , where $\sigma = [(N_{j-1} + N_{j+1})/2]^{1/2}$, the value of N_j is considered to be in error. Reflections containing intensity errors are preceded by ** in the final printout, and a separate table is printed, containing for each hkl the specific N_j 's (together with the corresponding position in $\Delta'\varphi$ units) in error. Corrections for linearity (obtained from the 'linearity' table by interpolation) are then made and the area less background obtained as in the preceding section. The absorption factor is then interpolated from the input table by the Aitken interpolation procedure. The Lorentz and polarization factors are computed directly from the values of ν and v .

The final printout includes the title, hkl , integrated intensity, absorption factor, Lorentz factor, polarization factor, extinction factor, F^2 , F , $\sigma(F^2)$, $\sigma(F)$, and the difference between the position of the principal maximum and the theoretical maximum in the intensity profile, in columns. An error indicator precedes each hkl . A blank corresponds to no error: a * to an intensity error; a ** to an angular error and a *** to both angular and intensity errors. Separate tables in the final printout contain, respectively, all the angle errors with both the observed and computed values, and the intensity errors with both the value and the position (in units of $\Delta'\varphi$) of the N_j in error. PEXRAD OUTPUT also produces punched cards containing the error indicators, hkl (based on the rotation axis arbitrarily named the c axis), $h'k'l'$ (transformed back to the standard cell), $F^2(hkl)$, and $\sigma^2(F^2(hkl))$. These cards are used by two additional PEXRAD programs which are described below.

† The availability of an IBM 1011 paper tape reader accessory for the IBM 1401 now permits much faster conversion from paper tape directly to magnetic tape.

Statistical analysis of PEXRAD structure amplitudes

PEXRAD OUTPUT computes magnitudes, variances, and standard deviations for every allowed hkl structure amplitude. The values of $F^2(hkl)$, $\sigma^2(F^2(hkl))$ and $\sigma(F^2(hkl))$ are independently measured for each of R equivalent positions.

A separate program reads the error indicators, hkl , $F^2(hkl)$, and $\sigma^2(F^2(hkl))$, and computes \bar{F}^2 , $\sigma^2\bar{F}^2$ and $\sigma\bar{F}^2$ using the formulae

$$\bar{F}^2 = \frac{1}{R} \sum_1^R F^2(hkl)_j,$$

$$\sigma^2(\bar{F}^2) = \frac{1}{R} \sum_1^R \sigma^2(F^2(hkl)_j).$$

And

$$\sigma(\bar{F}^2) = [\sigma^2(\bar{F}^2)]^{1/2}.$$

An additional measure of the variance in the mean structure amplitude is obtained from

$$V(\bar{F}^2) = \frac{\sum_{j=1}^R (F_j^2 - \bar{F}^2)^2}{R-1}.$$

The quantity $V(\bar{F}^2)$ estimates the systematic error as well as the precision in the counting statistics present in the equivalent reflections. In the absence of systematic error, the variance ratio $V(\bar{F}^2)/\sigma^2(\bar{F}^2)$ corresponds to the appropriate F -distribution for the number of degrees of freedom in the two variances. Both $V(\bar{F}^2)$ and the variance ratio are computed.

Finally, \bar{F} and $\sigma\bar{F}$ are obtained for use in subsequent crystallographic calculations, where $\bar{F} = (\bar{F}^2)^{1/2}$ and $\sigma\bar{F} = \sigma(\bar{F}^2)/2\bar{F}$.

PEXRAD balanced filter program

Current practice with PEXRAD uses balanced alpha and beta filters as well as pulse height discrimination to eliminate the harmonic contributions to the observed intensities. The structure factors and corresponding standard deviations obtained by this technique are computed in an additional short program using the relations

$$\bar{F}(hkl) = [\bar{F}^2(hkl)_\beta - \bar{F}^2(hkl)_\alpha]^{1/2}$$

and

$$\sigma^2\bar{F}^2(hkl) = \sigma^2\bar{F}^2(hkl)_\alpha + \sigma^2\bar{F}^2(hkl)_\beta,$$

where $\bar{F}^2(hkl)_{\alpha,\beta}$ and $\sigma^2\bar{F}^2(hkl)_{\alpha,\beta}$ refer to the previously averaged structure amplitudes and their variances measured respectively with the α , β filter.

IBM 7090 computation time

An important aspect of any program is the elapsed time in solving a typical problem. For PEXRAD INPUT, the complete calculation for 179 reflections distributed over 7 reciprocal layers took 0.0039 hour. For PEXRAD OUTPUT, the time taken to process

the same number of reflections is 0.0209 hour. Running time for the PEXRAD peripheral programs is small. In both INPUT and OUTPUT, printing time (on a 1401 machine) is additional to the times given.

It is a pleasure to thank Dr M. B. Wilk for valuable discussions of the standard deviation in the integrated intensity, Mrs G. Hansen for assistance with the FAP section of PEXRAD INPUT, Mr L. J. Cirincione for writing the IBM 1011 paper tape to magnetic tape program, and Mr J. L. Bernstein for running many calculations with these programs on the IBM 7090.

Note added in proof.— The K -values of N_j are no

longer necessarily used in calculating $I(hkl)$ and $\sigma^2(I(hkl))$. Now, the program integrates from the first ten 'good' background points on one side of the principal maximum to the first ten 'good' background points on the other side of the same maximum. If this criterion is not met, the program then uses all K points.

References

- ABRAHAMS, S. C. (1962). *Rev. Sci. Instrum.* **33**, 973.
 BOND, W. L. (1959). *International Tables for X-ray Crystallography*, II. Birmingham: Kynoch Press.
 BUEGER, M. J. (1960). *Crystal Structure Analysis*. New York: Wiley.
 PREWITT, C. T. (1960). *Z. Kristallogr.* **114**, 355.
 SAUTTER, J. (1961). Private communication.

Acta Cryst. (1963). **16**, 946

The Crystal Structure of α -Ga₂S₃

By J. GOODYEAR AND G. A. STEIGMANN

Department of Physics, The University, Hull, England

(Received 22 November 1962)

The structure of α -Ga₂S₃ has been determined from single-crystal and powder diffraction data. The unit cell is monoclinic, space group Cc , $a = 11.14_0$, $b = 6.41_1$, $c = 7.03_8$ Å, $\beta = 121.22^\circ$, and $Z = 4$. The structure, which is based on wurtzite with 4 cation vacancies per cell, differs from that proposed by Hahn & Frank mainly in the disposition of the vacant sites. Shrinkage of sulphur tetrahedra around these sites leads to some distortion from ideal close packing.

1. The unit cell and space group

The crystal structure of α -Ga₂S₃ was determined by Hahn & Frank (1955) as hexagonal, the sulphur atoms being in hexagonally close-packed layers perpendicular to the c axis and the gallium atoms filling some of the tetrahedral positions occupied by Zn in the wurtzite structure. Later, Goodyear, Duffin & Steigmann (1961) showed that the space lattice really has monoclinic symmetry, the unit cell being centred on the C face. They also pointed out that the lattice spacings observed by Hahn & Frank were in fact reconcilable with a rhombohedral cell closely related to their monoclinic cell.

Goodyear *et al.* found that their cell contained 4 molecules and, because of its shape and size, they concluded that the sulphur atoms must be nearly hexagonally close-packed in layers perpendicular to the $[101]$ axis. However, they did not consider the conventional and most convenient cell, which is formed by taking a new a axis along the $[102]$ direction, giving new cell parameters $a = 11.14_0$, $b = 6.41_1$, $c = 7.03_8$ Å, $\beta = 121.22^\circ$. The relation between the two cells is shown in Fig. 1; the conventional cell is still centred on the C face and the close-packed sulphur layers would now lie parallel to the (001) face.

A quantitative inspection of the intensities of the

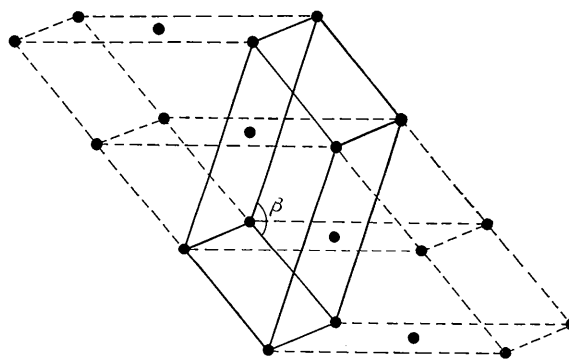


Fig. 1. The unit cell α -Ga₂S₃ (—— outline of conventional cell, ---- outline of cell chosen by Goodyear, Duffin & Steigmann).

spots on the b axis photographs indexed by Goodyear, Duffin & Steigmann has shown that the diffraction patterns were not strictly symmetrical about the zero layer line, indicating that the crystal was not oscillating about the true b axis. Consequently, these authors incorrectly indexed reflexions and assigned the structure to the wrong space group. Because of the near rhombohedral nature of the lattice, the $[110]$ and $[1\bar{1}0]$ directions in the conventional cell are